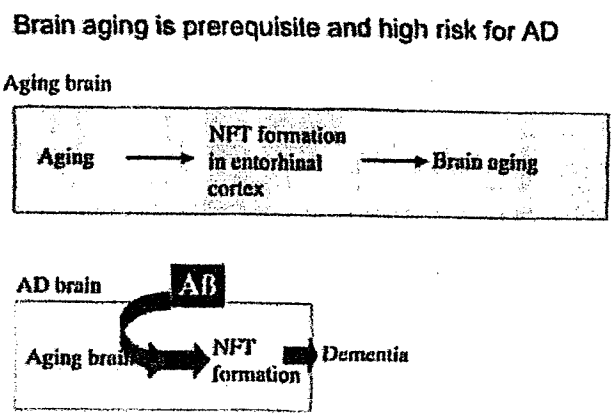

Fig. 3. Brain aging is a prerequisite and high risk factor for AD. During the aging process, normal aging induces NFT formation without the deposition of Aβ, leading to brain aging and mild cognitive impairment. In AD, the aging process is activated such that Aβ accelerates aging, leading to dementia through the spread of NFTs to limbic areas and neocortex. According to this scenario, Aβ is responsible for causing dementia in AD, and NFTs reflect the clinical course of AD.

ing factor may induce pathological changes in tau in entorhinal cortex, leading to memory impairment. In AD, Aβ may trigger pathological changes in tau in the limbic system and neocortex, leading to dementia. In clinically diagnosed AD, eliminating Aβ aggregation may be insufficient to block the progression of cognitive impairment in AD, because Aβ may have already initiated the tau aggregation cascade.

DISCLOSURE

Dr. Takashima receives funding from Abbott Laboratories.

REFERENCES

[1] Reisberg B, Ferris SH, de Leon MJ, Crook T (1982) The Global Deterioration Scale for assessment of primary degenerative dementia. *Am J Psychiatry* **139**, 1136-1139.

[2] Hardy J, Allsop D (1991) Amyloid deposition as the central event in the aetiology of Alzheimer's disease. *Trends Pharmacol Sci* **12**, 383-388.

[3] Hutton M, Perez-Tur J, Hardy J (1998) Genetics of Alzheimer's disease. *Essays Biochem* **33**, 117-131.

[4] Hardy J (2006) Alzheimer's disease: the amyloid cascade hypothesis: an update and reappraisal. *J Alzheimers Dis* **9** (3 Suppl), 151-153.

[5] Hardy J, Selkoe DJ (2002) The amyloid hypothesis of Alzheimer's disease: progress and problems on the road to therapeutics. *Science* **297**, 353-356.

[6] Hardy JA, Higgins GA (1992) Alzheimer's disease: the amyloid cascade hypothesis. *Science* **256**, 184-185.

[7] Yankner BA, Duffy LK, Kirschner DA (1990) Neurotrophic and neurotoxic effects of amyloid beta protein: reversal by tachykinin neuropeptides. *Science* **250**, 279-282.

[8] Busciglio J, Lorenzo A, Yeh J, Yankner BA (1995) beta-amyloid fibrils induce tau phosphorylation and loss of microtubule binding. *Neuron* **14**, 879-888.

[9] Lorenzo A, Yankner BA (1994) Beta-amyloid neurotoxicity requires fibril formation and is inhibited by congo red. *Proc Natl Acad Sci U S A* **91**, 12243-12247.

[10] Ashe KH (2001) Learning and memory in transgenic mice modeling Alzheimer's disease. *Learn Mem* **8**, 301-308.

[11] Morgan D (2003) Learning and memory deficits in APP transgenic mouse models of amyloid deposition. *Neurochem Res* **28**, 1029-1034.

[12] Delacourte A (2006) From physiopathology to treatment of Alzheimer's disease. *Rev Neurol (Paris)* **162**, 909-912.

[13] Yankner BA (1992) Commentary and perspective on studies of beta amyloid neurotoxicity. *Neurobiol Aging* **13**, 615-616.

[14] Lorenzo A, Razzaboni B, Weir GC, Yankner BA (1994) Pancreatic islet cell toxicity of amylin associated with type-2 diabetes mellitus. *Nature* **368**, 756-760.

[15] Cribbs DH, Pike CJ, Weinstein SL, Velazquez P, Cotman CW (1997) All-D-enantiomers of beta-amyloid exhibit similar biological properties to all-L-beta-amyloids. *J Biol Chem* **272**, 7431-7436.

[16] Yoshiike Y, Akagi T, Takashima A (2007) Surface structure of amyloid-beta fibrils contributes to cytotoxicity. *Biochemistry* **46**, 9805-9812.

[17] Glabe CG (2006) Common mechanisms of amyloid oligomer pathogenesis in degenerative disease. *Neurobiol Aging* **27**, 570-575.

[18] Look GC, Jerecic J, Cherbavaz DB, Pray TR, Breach JC, Crosier WJ, Igoudin L, Hironaka CM, Lowe RM, McEntee M, Ruslim-Litrus L, Wu HM, Zhang S, Catalano SM, Goure WF, Summa D, Krafft GA (2007) Discovery of ADDL – targeting small molecule drugs for Alzheimer's disease. *Curr Alzheimer Res* **4**, 562-567.

[19] Walsh DM, Klyubin I, Fadeeva JV, Rowan MJ, Selkoe DJ (2002) Amyloid-beta oligomers: their production, toxicity and therapeutic inhibition. *Biochem Soc Trans* **30**, 552-557.

[20] De Felice FG, Velasco PT, Lambert MP, Viola K, Fernandez SJ, Ferreira ST, Klein WL (2007) Abeta oligomers induce neuronal oxidative stress through an N-methyl-D-

aspartate receptor-dependent mechanism that is blocked by the Alzheimer drug memantine. *J Biol Chem* **282**, 11590-11601.

[21] Klein WL (2002) Abeta toxicity in Alzheimer's disease: globular oligomers (ADDLs) as new vaccine and drug targets. *Neurochem Int* **41**, 345-352.

[22] Wang HW, Pasternak JF, Kuo H, Ristic H, Lambert MP, Chromy B, Viola KL, Klein WL, Stine WB, Krafft GA, Trommer BL (2002) Soluble oligomers of beta amyloid (1-42) inhibit long-term potentiation but not long-term depression in rat dentate gyrus. *Brain Res* **924**, 133-140.

[23] Knobloch M, Farinelli M, Konietzko U, Nitsch RM, Mansuy IM (2007) Abeta oligomer-mediated long-term potentiation impairment involves protein phosphatase 1-dependent mechanisms. *J Neurosci* **27**, 7648-7653.

[24] Walsh DM, Klyubin I, Fadeeva JV, Cullen WK, Anwyl R, Wolfe MS, Rowan MJ, Selkoe DJ (2002) Naturally secreted oligomers of amyloid beta protein potently inhibit hippocampal long-term potentiation *in vivo*. *Nature* **416**, 535-539.

[25] Chapman PF (2000) Alzheimer's disease: model behaviour. *Nature* **408**, 915-916.

[26] Dodart JC, Bales KR, Gannon KS, Greene SJ, DeMattos RB, Mathis C, DeLong CA, Wu S, Wu X, Holtzman DM, Paul SM (2002) Immunization reverses memory deficits without reducing brain Abeta burden in Alzheimer's disease model. *Nat Neurosci* **5**, 452-457.

[27] Klyubin I, Walsh DM, Lemere CA, Cullen WK, Shankar GM, Betts V, Spooner ET, Jiang L, Anwyl R, Selkoe DJ, Rowan MJ (2005) Amyloid beta protein immunotherapy neutralizes Abeta oligomers that disrupt synaptic plasticity *in vivo*. *Nat Med* **11**, 556-561.

[28] McLaurin J, Cecal R, Kierstead ME, Tian X, Phinney AL, Manea M, French JE, Lambermon MH, Darabie AA, Brown ME, Janus C, Chishti MA, Horne P, Westaway D, Fraser PE, Mount HT, Przybylski M, St George-Hyslop P (2002) Therapeutically effective antibodies against amyloid-beta peptide target amyloid-beta residues 4-10 and inhibit cytotoxicity and fibrillogenesis. *Nat Med* **8**, 1263-1269.

[29] Morgan D, Diamond DM, Gottschall PE, Ugen KE, Dickey C, Hardy J, Duff K, Jantzen P, DiCarlo G, Wilcock D, Connor K, Hatcher J, Hope C, Gordon M, Arendash GW (2000) A beta peptide vaccination prevents memory loss in an animal model of Alzheimer's disease. *Nature* **408**, 982-985.

[30] Younkin SG (2001) Amyloid beta vaccination: reduced plaques and improved cognition. *Nat Med* **7**, 18-19.

[31] Holmes C, Boche D, Wilkinson D, Yadegarfar G, Hopkins V, Bayer A, Jones RW, Bullock R, Love S, Neal JW, Zotova E, Nicoll JA (2008) Long-term effects of Abeta42 immunisation in Alzheimer's disease: follow-up of a randomised, placebo-controlled phase I trial. *Lancet* **372**, 216-223.

[32] Roberson ED, Scearce-Levie K, Palop JJ, Yan F, Cheng IH, Wu T, Gerstein H, Yu GQ, Mucke L (2007) Reducing endogenous tau ameliorates amyloid beta-induced deficits in an Alzheimer's disease mouse model. *Science* **316**, 750-754.

[33] Gomez-Isla T, Hollister R, West H, Mui S, Growdon JH, Petersen RC, Parisi JE, Hyman BT (1997) Neuronal loss correlates with but exceeds neurofibrillary tangles in Alzheimer's disease. *Ann Neurol* **41**, 17-24.

[34] Spillantini MG, Goedert M (1998) Tau protein pathology in neurodegenerative diseases. *Trends Neurosci* **21**, 428-433.

[35] Hutton M (2001) Missense and splice site mutations in tau associated with FTDP-17: multiple pathogenic mechanisms. *Neurology* **56** (11 Suppl 4), 21-25.

[36] Hutton M (2000) Molecular genetics of chromosome 17 tauopathies. *Ann N Y Acad Sci* **920**, 63-73.

[37] Ingram EM, Spillantini MG (2002) Tau gene mutations: dissecting the pathogenesis of FTDP-17. *Trends Mol Med* **8**, 555-562.

[38] Goedert M, Spillantini MG (2000) Tau mutations in frontotemporal dementia FTDP-17 and their relevance for Alzheimer's disease. *Biochim Biophys Acta* **1502**, 110-121.

[39] van Swieten JC, Rosso SM, van Herpen E, Kamphorst W, Ravid R, Heutink P (2004) Phenotypic variation in frontotemporal dementia and parkinsonism linked to chromosome 17. *Dement Geriatr Cogn Disord* **17**, 261-264.

[40] Braak H, Braak E (1996) Evolution of the neuropathology of Alzheimer's disease. *Acta Neurol Scand Suppl* **165**, 3-12.

[41] Samuel W, Masliah E, Hill LR, Butters N, Terry R (1994) Hippocampal connectivity and Alzheimer's dementia: effects of synapse loss and tangle frequency in a two-component model. *Neurology* **44**, 2081-2088.

[42] Callahan LM, Selski DJ, Mantzen MR, Cheetham JE, Coleman PD (1994) Preliminary evidence: decreased GAP-43 message in tangle-bearing neurons relative to adjacent tangle-free neurons in Alzheimer's disease parahippocampal gyrus. *Neurobiol Aging* **15**, 381-386.

[43] Sato-Harada R, Okabe S, Umeyama T, Kanai Y, Hirokawa N (1996) Microtubule-associated proteins regulate microtubule function as the track for intracellular membrane organelle transports. *Cell Struct Funct* **21**, 283-295.

[44] Stamer K, Vogel R, Thies E, Mandelkow E, Mandelkow EM (2002) Tau blocks traffic of organelles, neurofilaments, and APP vesicles in neurons and enhances oxidative stress. *J Cell Biol* **156**, 1051-1063.

[45] Thies E, Mandelkow EM (2007) Missorting of tau in neurons causes degeneration of synapses that can be rescued by the kinase MARK2/Par-1. *J Neurosci* **27**, 2896-2907.

[46] Dixit R, Ross JL, Goldman YE Holzbaur EL (2008) Differential regulation of dynein and kinesin motor proteins by tau. *Science* **319**, 1086-1089.

[47] Morfini G, Pigino G, Mizuno N, Kikkawa M, Brady ST (2007) Tau binding to microtubules does not directly affect microtubule-based vesicle motility. *J Neurosci Res* **85**, 2620-2630.

[48] Ishihara T, Hong M, Zhang B, Nakagawa Y, Lee MK, Trojanowski JQ, Lee VM (1999) Age-dependent emergence and progression of a tauopathy in transgenic mice overexpressing the shortest human tau isoform. *Neuron* **24**, 751-762.

[49] Yuan A, Kumar A, Peterhoff C, Duff K, Nixon RA (2008) Axonal transport rates *in vivo* are unaffected by tau deletion or overexpression in mice. *J Neurosci* **28**, 1682-1687.

[50] Santacruz K, Lewis J, Spires T, Paulson J, Kotilinek L, Ingelsson M, Guimaraes A, DeTure M, Ramsden M, McGowan E, Forster C, Yue M, Orne J, Janus C, Mariash A, Kuskowski M, Hyman B, Hutton M, Ashe KH (2005) Tau suppression in a neurodegenerative mouse model improves memory function. *Science* **309**, 476-481.

[51] Spires-Jones TL, de Calignon A, Matsui T, Zehr C, Pitstick R, Wu HY, Osetek JD, Jones PB, Bacskai BJ, Feany MB, Carlson GA, Ashe KH, Lewis J, Hyman BT (2008) *In vivo* imaging reveals dissociation between caspase activation and acute neuronal death in tangle-bearing neurons. *J Neurosci* **28**, 862-867.

[52] Maeda S, Sahara N, Saito Y, Murayama M, Yoshiike Y, Kim H, Miyasaka T, Murayama S, Ikai A, Takashima A (2007) Granular tau oligomers as intermediates of tau filaments. *Biochemistry* **46**, 3856-3861.

[53] Maeda S, Sahara N, Saito Y, Murayama S, Ikai A, Takashima (2006) A Increased levels of granular tau oligomers: an early

sign of brain aging and Alzheimer's disease. *Neurosci Res* 54, 197-201.

[54] Engel T, Goni-Oliver P, Lucas JJ, Avila J, Hernandez F (2006) Chronic lithium administration to FTDP-17 tau and GSK-3beta overexpressing mice prevents tau hyperphosphorylation and neurofibrillary tangle formation, but pre-formed neurofibrillary tangles do not revert. *J Neurochem* 99, 1445-1455.

[55] Noble W, Planel E, Zehr C, Olm V, Meyerson J, Suleman F, Gaynor K, Wang L, LaFrancois J, Feinstein B, Burns M, Krishnamurthy P, Wen Y, Bhat R, Lewis J, Dickson D, Duff K (2005) Inhibition of glycogen synthase kinase-3 by lithium correlates with reduced tauopathy and degeneration *in vivo*. *Proc Natl Acad Sci U S A* 102, 6990-6995.

[56] Wischik CM, Bentham P, Wischik DJ, Seng KM (2008) Tau aggregation inhibitor (TAI) therapy with REMBER^{TM} arrests disease progression in mild and moderate Alzheimer's disease over 50 weeks. *Alzheimers Dement* 4 (Suppl), T167.

[57] Lee HG, Perry G, Moreira PI, Garrett MR, Liu Q, Zhu X, Takeda A, Nunomura A, Smith MA (2005) Tau phosphorylation in Alzheimer's disease: pathogen or protector? *Trends Mol Med* 11, 164-169.

THE PRODUCTION RATIOS OF AICDε51 AND Aβ42 BY INTRAMEMBRANE PROTEOLYSIS OF βAPP DO NOT ALWAYS CHANGE IN PARALLEL

Kohji MORI,[1)] Masayasu OKOCHI,[¶, 1)] Shinji TAGAMI,[1)] Taisuke NAKAYAMA,[1)] Kanta YANAGIDA,[1)] Takashi S. KODAMA,[1)] Shin-ichi TATSUMI,[1)] Kana FUJII, [1)] Hitoshi TANIMUKAI, [1)] Ryota HASHIMOTO, [1)] Takashi MORIHARA, [1)] Toshihisa TANAKA, [1)] Takashi KUDO [1)], Satoru FUNAMOTO,[2)] Yasuo IHARA[2)] and Masatoshi TAKEDA[1)]

[1)]Psychiatry, Department of Integrated Medicine, Division of Internal Medicine, Osaka University Graduate School of Medicine D3 2-2 Yamadaoka, Suita, Osaka 565-0871, and [2)]Department of Neuropathology, Faculty of Life and Medical Sciences, Doshisha University, 4-1-1, Kizugawadai, Kizugawa, Kyoto 619-0225, Japan

[¶]Senior author for correspondence:
Masayasu Okochi, M.D.
Psychiatry
Department of Integrated Medicine
Division of Internal Medicine
Osaka University Graduate School of Medicine
D3 2-2 Yamadaoka, Osaka 565-0871, Japan.
Email: mokochi@psy.med.osaka-u.ac.jp

RUNNING TITLE
Variety of ε-cleavage of βAPP

Abstract

Background: During intramembrane proteolysis of βAPP by presenilin (PS)/γ-secretase, ε-cleavages at the membrane-cytoplasmic border precede γ-cleavages at the middle of the transmembrane domain. Generation ratios of Aβ42, a critical molecule for Alzheimer disease (AD) pathogenesis, and the major Aβ40 species may be associated with ε48 and ε49 cleavages, respectively. Medicines to down-regulate Aβ42 production have been investigated by many pharmaceutical companies. Therefore, the ε-cleavages, rather than the γ-cleavage, may be more effective upstream targets for decreasing the relative generation of Aβ42. Thus, one may evaluate compounds by analyzing the generation ratio of the AICD species (ε-cleavage-derived), instead of that of Aβ42.

Methods: Cell-free γ-secretase assays were performed to observe *de novo* AICD production. Immunoprecipitation/MALDI-TOF MS analysis was performed to detect the N-termini of AICD species. Aβ and AICD species were measured by ELISA and immunoblotting techniques.

Results: Effects on the ε-cleavage by AD-associated pathological mutations around the ε-cleavage sites (*i.e.*, βAPP V642I, L648P and K649N), were analyzed. The V642I and L648P mutations caused an increase in the relative ratio of ε48 cleavage as expected from previous reports. Cells expressing the K649N mutant, however, underwent a major ε-cleavage at the ε51 site. These results suggest that ε51, as well as ε48 cleavage, is associated with Aβ42 production. Only AICDε51, though, and not Aβ42 production, dramatically changed with modifications to the cell-free assay conditions. Interestingly, the increase in the relative ratio of the ε51 cleavage by the K649N mutation was not cancelled by these changes.

Conclusion: Our current data indicate that the generation ratio of AICDε51 and Aβ42 do not always change in parallel. Thus, to identify compounds that decrease the relative ratio of Aβ42 generation, measurement of the relative level of Aβ42-related AICD species (*i.e.*, AICDε48 and AICDε51) might not be useful. Further studies to reveal how the ε-cleavage precision is decided are necessary before it will be possible to develop drugs targeting ε-cleavage as a means for decreasing Aβ42 production.

Key words: Alzheimer Disease, βAPP, γ-cleavage, ε-cleavage, presenilin/γ-secretase, "dual-cleavage" mechanism, AICDε51

INTRODUCTION

The transmembrane domain of β-Amyloid Protein Precursor (βAPP) is proteolysed by presenilin (PS)/γ-secretase [1]. Analysis of the resultant products has revealed that the proteolysis proceeds by at least two-distinct cleavages. The "ε-cleavage" liberates its intracellular domain (*i.e.*, AICD) into the cytoplasm, while the "γ-cleavage" releases Alzheimer disease (AD)-associated Amyloid β-protein (Aβ) [2-6].

There are some variations in both the γ- and ε-cleavages of βAPP [6-8]. The major N-termini of AICD species consist of leucine-49, valine-50 and leucine-52 (Aβ-numbering), while the major C-termini of Aβ species are comprised of valine-40 and alanine-42. (Figure 1A) [6]. Among these, highly aggregatable Aβ42 is the major component of senile plaques in AD brains [9].

Are there any relationships between the ε- and γ-cleavages? How do these cleavages occur? Ihara and colleagues have tried to address these questions and recently revealed that ε-cleavage precedes γ-cleavage in *in vitro* γ-secretase assays [10]. βAPP-CTF stubs, βAPP membrane-tethered remnants following β-cleavage, first undergo ε-cleavage [10]. The ε-cleavage liberates AICD from the membrane and produces a membrane-bound 48/49 amino-acid-long Aβ species that undergoes further C-terminal truncation by PS/γ-secretase [11]. Stepwise cleavages remove every three amino-acid residues from the C-terminus of the long Aβ species, which finally secretes Aβ40/42 [12-14]. For example, mutant PS causes increased both ε48 and γ42 cleavages [8]. Thus, the γ-cleavage seems to occur in an ε-cleavage-dependent manner [10]. Moreover, these results indicate that the production process for pathological Aβ42 is distinct from that of Aβ40 [15]. That is, the major ε49 cleavage causes the production of Aβ40, while a minor ε48 cleavage causes production of pathological Aβ42 [14].

Modulation of γ-secretase function to specifically inhibit Aβ42 production is one of the promising strategies for developing drugs to modify the disease course of AD [16]. Given the possible correlation between the ε- and γ-cleavages, we think that targeting the up-stream ε-cleavages will be a novel and more efficient method for developing Aβ42-lowering drugs. To test if precision of the ε-cleavage can be used as a novel target for drug development, we investigated the ε-cleavage pathway, particularly ε51 cleavage, which has previously not been well-characterized [7].

RESULTS

The βAPP K649N Belgian mutant increased both the relative ratio of AICDε51 and Aβ42 production in a cell-free γ-secretase assay.

To test if the ε51 cleavage precedes the γ42 cleavage, we analyzed the effects of three βAPP mutants (V642I [17], L648P [18], and K649N [19]) around the ε-site. The L648P and K649N mutants (βAPP695 numbering) are located downstream of the ε51 site, and the V642I mutant is located upstream of the ε48 site (Figure 1A). Each of the three mutants is familial AD-associated and, therefore, increases the relative ratio of Aβ42 production. We raised K293 cells stably expressing each of the mutants, prepared the crude membrane fractions [20] and performed the cell-free γ-secretase assays [7,21].

As shown in Figure 1B, the K649N βAPP mutant caused marked increase in the relative ratio of AICDε51 production. However, the other two mutants caused completely different effects on the cleavage. The L648P mutant produced a barely detectable level of AICDε51, while in the V642I mutant cells, the ratio of AICDε51 production was comparable to that of wild-type (wt) expressing cells. It is of note that, instead of increased AICDε51 production, these V642I and L648P mutants substitutively increased the relative ratio of AICDε48 production. Next we measured Aβ species secretion by the stable cells in conditioned media using ELISA (Figure 1C). As expected, we observed a significant increase in the ratio of Aβ42 to total Aβ secretion in the conditioned medium of the mutant cells. This data indicates that the K649N mutant increased the ratio of Aβ42 production through up-regulation of the ε51 cleavage, while the V642I and L648P mutants increased Aβ42 production through the ε48 cleavage. Based on these results, we suggest that not only the ε48 but also the ε51 cleavage precedes Aβ42 production, possibly by sequential three amino-acid C-terminal truncation [14] (Figure 1D).

Incubation in higher pH does not cancel the K649N βAPP mutant effects.

We previously found that the precision of ε-cleavage changes depending on the buffer pH [7,21]. The relative ratio of AICDε51 production is the most sensitive to such changes. Therefore, we next determined whether the relative ratio of AICDε51 and/or Aβ42 production by the K649N mutant is affected by changing the buffer pH during the cell-free assay. As expected, incubation in the higher pH (pH 7.4 vs pH 6.0) buffer decreased the relative ratio of AICDε51 generation in both the K649N mutant and wt βAPP membrane fraction. However, the pH effect was not so strong as to cancel the AICDε51 up-regulation effect by the K649N mutant (Figure 2A). We further analyzed the pH effects on the increase in the relative ratio of Aβ42 production by the mutant

(Figure 2B). Surprisingly, the assay pH elevation did not cause any changes in the relative ratio of Aβ42 generation. Therefore, unlike the effects of the K649N mutant on the ε51- and γ42-cleavages, the elevation of the buffer pH causes a decrease in the relative ratio of AICDε51 production but does not cause any changes in Aβ42 production. The data suggests that two distinct mechanisms may contribute to the determination of the relative ratio of AICDε51 production.

Alkali pre-treatment of the crude membrane fraction cancels the effect of higher pH cell-free incubation on ε-cleavage.

Since the ε51 cleavage occurs at the membrane-cytosol interface, we considered that membrane-bound substances might induce the pH-dependent effects on AICDε51 production. Many substances detach from the membrane upon treatment with alkali solution [22]. To test this theory, we washed the wt βAPP membrane fraction in a pH 11 solution (see "Materials and Methods") then conducted the cell-free assay at pH 6.0. The relative ratio of AICDε51 production markedly decreased (Figure 3A), while that of the Aβ42 did not (Figure 3B). The phenomena are reminiscent of the effects of raising the pH of the incubation buffer (see Figure 2). Thus, we further considered that the decrease in the AICDε51 production resulting from the use of a higher incubation buffer pH might also be due to detachment of substances from the membrane. When the membrane fraction was incubated in a pH 7.4 buffer after alkali treatment, we could no longer observe the pH-dependent incubation buffer effects on the AICDε51 ratio (Figure 3C). Collectively, though incubation at lower pH buffer increased in the AICDε51 ratio (Figure 2A), the effects was cancelled by the alkali pre-treatment (Figure 3A). These results suggest that substances removed by the alkali treatment might induce the changes in the relative ratio of AICDε51 production.

Alkali pre-treatment of the crude membrane fraction did not cancel the effects of the K649N mutant on the ε-cleavage.

As shown in Figure 1, the K649N βAPP mutation causes up-regulation of both the AICDε51 and Aβ42 ratio, while alkali pre-treatment causes down-regulation of only the AICDε51 ratio (Figure 3). These data indicate that changes in the AICDε51 ratio caused by the mutation and by the treatment occur by two distinct processes. A further experiment was conducted to confirm whether the K649N mutation cause a change in the relative ratio of AICDε51 production through the effect of the alkali treatment (Figure 4A). Following treatment of the K649N mutant membrane fraction in the alkali solution, the cell-free assay was performed at pH 6.0. As shown in Figure

4A, even after the alkali treatment, the K649N mutant membrane produced a relatively higher level of AICDε51 than that of the wt fraction (Figure 3A). Moreover, the elevated Aβ42 ratio was not changed by the pre-treatment (Figure 4B).

DISCUSSION

In the present study we determined that there are at least two factors that change the precision of ε-cleavage: (i) a process induced by a pathological βAPP mutation and (ii) another process induced by possibly unidentified substances removed from the membrane fraction by alkali pre-treatment. In the case of βAPP mutations, the relative ratio of ε51 and ε48 production increases in parallel with the ratio of AD-associated Aβ42.

It has been reported that ε-cleavage precedes γ-cleavage and γ-cleavage seems to occur in an ε-cleavage-dependent manner [10]. Considering these reports and our own preliminary results, it seemed possible that measurement of the relative ratio of AICDε48/AICDε51 production might help develop Aβ42-lowering anti-AD drugs. Further study revealed, however, that the relative level of AICDε51 production is drastically affected by the removal of unidentified substances from the membrane as a result of alkali pre-treatment. Interestingly, the alkali pre-treatment did not cause any changes in the relative ratio of Aβ42 generation. These results indicate that changes in the precision of ε-cleavage do not always cause parallel alterations in the precision of γ-cleavage, even though ε-cleavage occurs upstream of the γ-cleavage. Therefore, although measuring the levels of AICD species is a potentially attractive new target for developing Aβ42 lowering compounds, challenges still must be overcome before screening methods for such compounds can be established. For example, the paradoxical mechanism discussed above must first be understood before an assay in which the ε-cleavage precision accurately reflects the γ-cleavage precision can be developed.

How does alkali pre-treatment result in a decreased ratio of AICDε51 production? One may consider the presence of unknown substances which (i) transiently associate with the PS/γ-secretase and affect its intramembrane cleavage precision, or (ii) truncate a couple of N-terminal amino-acid residues of AICD produced by the ε-cleavage. The second possibility is reminiscent of ACE activity to truncate the C-terminus of Aβ42 [23]. Of course, the possibility that alkali pre-treatment might change the character of PS/γ-secretase itself also cannot be excluded.

CONCLUSION

Our current data suggest that the precision of ε-cleavage do not always changes in parallel with the precision of γ-cleavage, even though ε-cleavage occurs upstream of the γ-cleavage. Thus, to measure the levels of AICD species might be an attractive new target for developing Aβ42 lowering compounds, there still remain some

challenges.

MATERIALS AND METHODS

Cell culture and cDNA constructs

cDNAs of βAPP V642I, L648P and K649N mutants were generated by PCR-based mutagenesis using a Quickchange mutagensis kit (Stratagene) or KOD plus (Toyobo) with wt βAPP695 cDNA as a template. K293 cells were transfected and cultured as previously described [24].

Membrane preparation

The crude membrane fraction was prepared as previously described with a slight modification [7,21]. In the present study, the homogenization buffer contained 0.25 M sucrose and 50 mM HEPES (pH 7.4) containing a protease inhibitor cocktail (Roche). To prepare the alkaline pre-treated membrane, the membrane fraction was suspended in a 50 mM bicarbonate buffer (pH 11.0) and incubated at 4 °C for 1 h. The suspension was then centrifuged at 100,000 × g for 1 h followed by washing once with a 50 mM Mes buffer (pH 6.0).

Cell-free γ-secretase assay

The cell-free γ-secretase assay was performed as previously described with a modification [7,21]. The reaction buffer in the present study contained a 150 mM citrate buffer (pH 6.0), 50 mM MES (pH 6.0), 167 mM NaCl and a protease inhibitor mixture comprised a 5x complete protease inhibitor cocktail (Roche), 0.5 mM DIFP (WAKO), 1 μg/ml TLCK (Sigma-Aldrich), 10 μg/ml antipain (Peptide Institute), 10 μg/ml leupeptin (Peptide Institute), 5 mM 1,5 phenanthroline (Sigma-Aldrich), 10 μM amastatin (Peptide Institute), 10 μM bestatin (WAKO), 1 μM thiorphan (Sigma-Aldrich), 10 μM phosphoramidon (Peptide Institute) and 1 μM pepstatin A (Peptide Institute). To prepare the pH 7.4 buffer, 50 mM HEPES (pH 7.4) was used instead of the citrate and MES buffers.

Immunoprecipitation/MALDI MS (IP-MS) analysis

IP-MS analysis followed by cell-free incubation was carried out as previously described [7,21,25]. The heights of the MS peaks and molecular weights were calibrated using angiotensin and bovine insulin β-chain as standards (Sigma-Aldrich).

ELISA analysis for Aβ

Aβ40 and Aβ42 levels in conditioned media were quantified by ELISA (WAKO).

Immunoblotting of Aβ

SDS-solubilized proteins were separated by SDS-PAGE using an 8 M Urea gel [24] and transferred to a nitrocellulose membrane. Immunoblotting of Aβ species using 82E1 (IBL) was performed as previously described [26].

ACKNOWLEDGEMENTS

M.O. and coworkers are funded by the National Institute of Biomedical Innovation (05-26), the Ministry of Education, Culture, Sports, Science and Technology, and the Ministry of Health, Labor and Welfare, Japan.

The authors declare no competing financial interests.

REFERENCES

1. Wolfe MS, Xia W, Ostaszewski BL, Diehl TS, Kimberly WT, Selkoe DJ. Two transmembrane aspartates in presenilin-1 required for presenilin endoproteolysis and gamma-secretase activity. *Nature* 1999;**398**:513-7.
2. Gu Y, Misonou H, Sato T, Dohmae N, Takio K, Ihara Y. Distinct intramembrane cleavage of the beta-amyloid precursor protein family resembling gamma-secretase-like cleavage of Notch. *J Biol Chem* 2001;**276**:35235-8.
3. Sastre M, Steiner H, Fuchs K, et al. Presenilin-dependent gamma-secretase processing of beta-amyloid precursor protein at a site corresponding to the S3 cleavage of Notch. *EMBO Rep* 2001;**2**:835-41.
4. Yu C, Kim SH, Ikeuchi T, et al. Characterization of a presenilin-mediated amyloid precursor protein carboxyl-terminal fragment gamma. Evidence for distinct mechanisms involved in gamma -secretase processing of the APP and Notch1 transmembrane domains. *J Biol Chem* 2001;**276**:43756-60.
5. Chen F, Gu Y, Hasegawa H, et al. Presenilin 1 mutations activate gamma 42-secretase but reciprocally inhibit epsilon-secretase cleavage of amyloid precursor protein (APP) and S3-cleavage of notch. *J Biol Chem* 2002;**277**:36521-6.
6. Selkoe DJ. Alzheimer's disease: genes, proteins, and therapy. *Physiol Rev* 2001;**81**:741-66.
7. Fukumori A, Okochi M, Tagami S, et al. Presenilin-dependent gamma-secretase on plasma membrane and endosomes is functionally distinct. *Biochemistry* 2006;**45**:4907-14.
8. Sato T, Dohmae N, Qi Y, et al. Potential link between amyloid beta-protein 42 and C-terminal fragment gamma 49-99 of beta-amyloid precursor protein. *J Biol Chem*

2003;278:24294-301.

9. Iwatsubo T, Odaka A, Suzuki N, Mizusawa H, Nukina N, Ihara Y. Visualization of A beta 42(43) and A beta 40 in senile plaques with end-specific A beta monoclonals: evidence that an initially deposited species is A beta 42(43). *Neuron* 1994;13:45-53.
10. Kakuda N, Funamoto S, Yagishita S, et al. Equimolar production of amyloid beta-protein and amyloid precursor protein intracellular domain from beta-carboxyl-terminal fragment by gamma-secretase. *J Biol Chem* 2006;281:14776-86.
11. Funamoto S, Morishima-Kawashima M, Tanimura Y, Hirotani N, Saido TC, Ihara Y. Truncated carboxyl-terminal fragments of beta-amyloid precursor protein are processed to amyloid beta-proteins 40 and 42. *Biochemistry* 2004;43:13532-40.
12. Qi-Takahara Y, Morishima-Kawashima M, Tanimura Y, et al. Longer forms of amyloid beta protein: implications for the mechanism of intramembrane cleavage by gamma-secretase. *J Neurosci* 2005;25:436-45.
13. Yagishita S, Morishima-Kawashima M, Tanimura Y, Ishiura S, Ihara Y. DAPT-induced intracellular accumulations of longer amyloid beta-proteins: further implications for the mechanism of intramembrane cleavage by gamma-secretase. *Biochemistry* 2006;45:3952-60.
14. Takami M, Nagashima Y, Sano Y, et al. gamma-Secretase: successive tripeptide and tetrapeptide release from the transmembrane domain of beta-carboxyl terminal fragment. *J Neurosci* 2009;29:13042-52.
15. Yagishita S, Morishima-Kawashima M, Ishiura S, Ihara Y. Abeta46 is processed to Abeta40 and Abeta43, but not to Abeta42, in the low density membrane domains. *J Biol Chem* 2008;283:733-8.
16. Weggen S, Eriksen JL, Das P, et al. A subset of NSAIDs lower amyloidogenic Abeta42 independently of cyclooxygenase activity. *Nature* 2001;414:212-6.
17. Goate A, Chartier-Harlin MC, Mullan M, et al. Segregation of a missense mutation in the amyloid precursor protein gene with familial Alzheimer's disease. *Nature* 1991;349:704-6.
18. Kwok JB, Li QX, Hallupp M, et al. Novel Leu723Pro amyloid precursor protein mutation increases amyloid beta42(43) peptide levels and induces apoptosis. *Ann Neurol* 2000;47:249-53.
19. Theuns J, Marjaux E, Vandenbulcke M, et al. Alzheimer dementia caused by a novel mutation located in the APP C-terminal intracytosolic fragment. *Hum Mutat* 2006;27:888-96.
20. Pinnix I, Musunuru U, Tun H, et al. A novel gamma -secretase assay based on detection of the putative C-terminal fragment-gamma of amyloid beta protein precursor. *J*

Biol Chem 2001;**276**:481-7.

21. Tagami S, Okochi M, Yanagida K, et al. Regulation of notch signaling by dynamic changes in the precision of s3 cleavage of notch-1. *Mol Cell Biol* 2008;**28**:165-76.
22. Hubbard AL, Wall DA, Ma A. Isolation of rat hepatocyte plasma membranes. I. Presence of the three major domains. *J Cell Biol* 1983;**96**:217-29.
23. Zou K, Yamaguchi H, Akatsu H, et al. Angiotensin-converting enzyme converts amyloid beta-protein 1-42 (Abeta(1-42)) to Abeta(1-40), and its inhibition enhances brain Abeta deposition. *J Neurosci* 2007;**27**:8628-35.
24. Okochi M, Fukumori A, Jiang J, et al. Secretion of the Notch-1 Abeta-like peptide during Notch signaling. *J Biol Chem* 2006;**281**:7890-8.
25. Okochi M, Steiner H, Fukumori A, et al. Presenilins mediate a dual intramembranous gamma-secretase cleavage of Notch-1. *Embo J* 2002;**21**:5408-16.
26. Yanagida K, Okochi M, Tagami S, et al. The 28-amino acid form of an APLP1-derived Abeta-like peptide is a surrogate marker for Abeta42 production in the central nervous system. *EMBO Mol Med* 2009;**1**:223-35.

FIGURE LEGENDS

Figure 1. Effect of familial AD-associated βAPP mutations around the ε-cleavage site.

A, Schematic diagram of intramembrane cleavage sites of βAPP and the familial AD mutations used in the present study. The amino acid sequence around the juxta membrane region of human βAPP is described (Aβ numbering). Filled inverted triangles indicate the cleavage sites. Substituted amino acids of the familial AD mutations are indicated in open rectangles. The site of each mutant is also indicated using APP695 numbering.

B, Mass spectra of *de novo* AICD species in the cell-free assay. Crude membrane fractions obtained from wt βAPP and the indicated βAPP mutant cells were used.

C, Relative secreted Aβ42 to Aβ40 ratio in the conditioned media of wt βAPP and the indicated βAPP mutant cells. The asterisks indicate statistical significance (*P<0.05, **P<0.001, one-way analysis of variance (ANOVA) and Tukey-Kramer method). Error bars indicate standard error of the mean (SEM).

D, Hypothesis for explaining increased γ42 cleavage in each mutant βAPP (upper panels) and differential production of Aβ40 and Aβ42 (lower panels).

Figure 2. Effect of cell-free incubation pH levels on the precision of ε/γ-cleavages.

A, Mass spectra of AICD generated in the cell-free assay performed at the indicated pH (upper and middle panels). Peak heights of AICDε49 and ε51 were measured and the ratios of AICDε49 to ε51 were calculated (lower panel). The asterisks indicate statistical significance (*P<0.05, **P<0.001, one-way ANOVA and Tukey-Kramer method). Error bars indicate SEM.

B, Levels of Aβ generated at the indicated pH. Levels of Aβ40 and 42 were measured by western blotting and the Aβ42 to 40 ratios calculated. The asterisks indicate statistical significance. Error bars show SEM.

Figure 3. Effect of alkali pre-treatment on the precision of ε/γ-cleavages of wt βAPP.

A, Mass spectra of AICD generated in the cell-free assay with and without alkali pre-treatment. Peak heights of AICDε49 and ε51 were measured and the AICDε49 to ε51 ratios calculated. The asterisk indicates statistical significance (*P<0.05, paired t-test). Error bars indicate SEM.

B, Levels of Aβ generated in the cell-free assay following alkali pre-treatment. Levels of Aβ40 and 42 were measured by western blotting with and without alkali pre-treatment and the Aβ42 to 40 ratios calculated.

C, Mass spectra of AICD generated in the cell-free assay at the indicated pH following

alkali pre-treatment.

Figure 4. Effect of alkali pre-treatment on the precision of ε/γ-cleavages of βAPP K649N Belgian mutant.

A, Mass spectra of AICD generated in the cell-free assay with and without alkali pre-treatment.

B, Levels of Aβ generated in the cell-free assay following alkali pre-treatment.

Table 1. **Molecular species of AICD generated in the cell-free assay.**

AICD species		m/z		
		Calculated [M+H]	observed [M+H]	
			mean	SD
AICDε51 (52-99)	wt	5677.79	5678.38	0.64
	V642I	5677.79	5678.30	0.70
	K649N	5663.74	5663.96	0.23
AICDε49 (50-99)	wt	5907.9	5908.35	0.29
	V642I	5907.9	5908.49	0.21
	L648P	5891.87	5892.48	0.20
	K649N	5893.84	5894.10	0.27
AICDε48 (49-99)	wt	6020.98	6021.36	0.40
	V642I	6020.98	6021.59	0.42
	L648P	6004.96	6005.59	0.33
	K649N	6006.93	6007.51	0.17
AICDε52 (53-99)	K649N	5550.65	5551.01	0.27

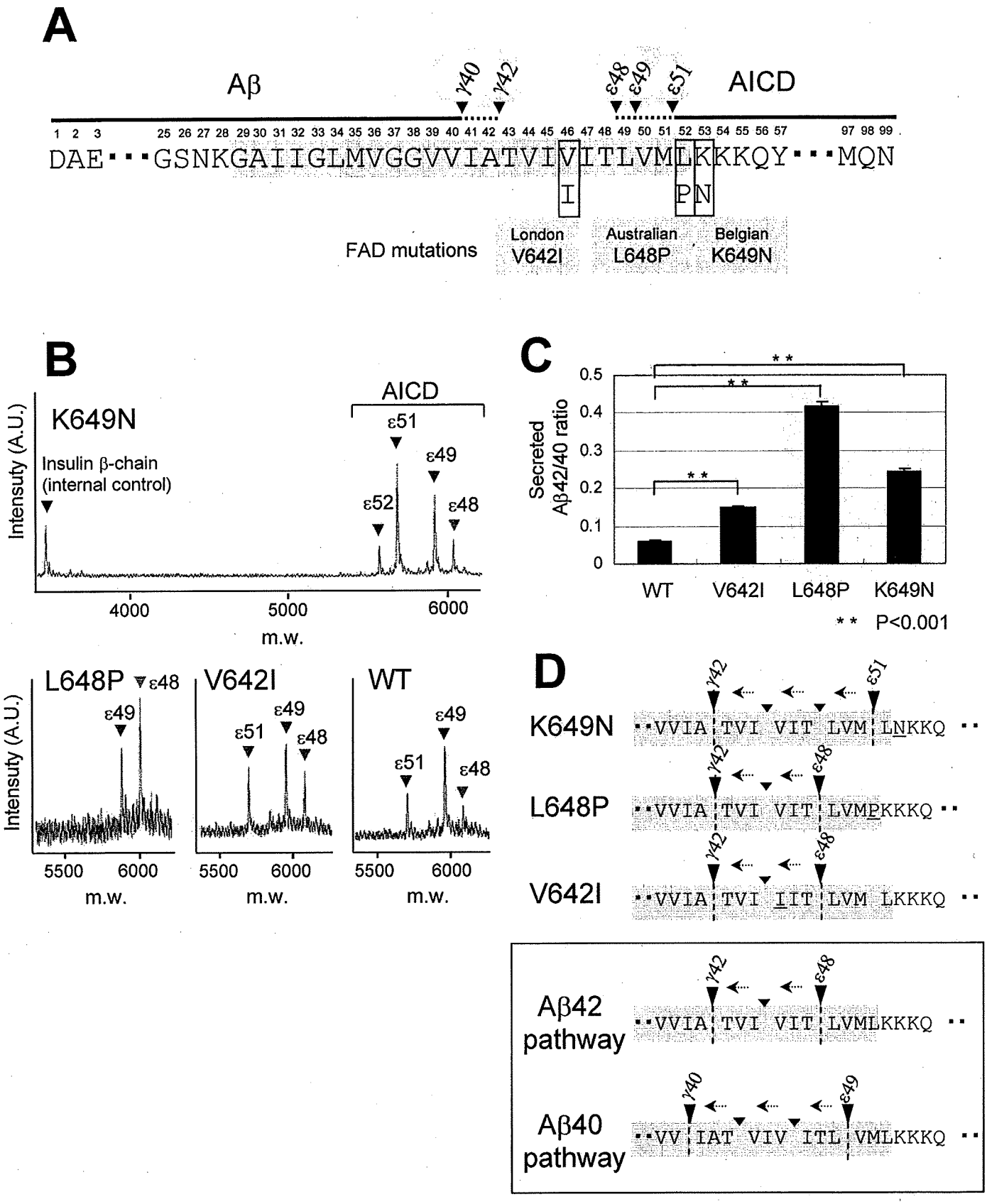

Mori et al., Figure 1

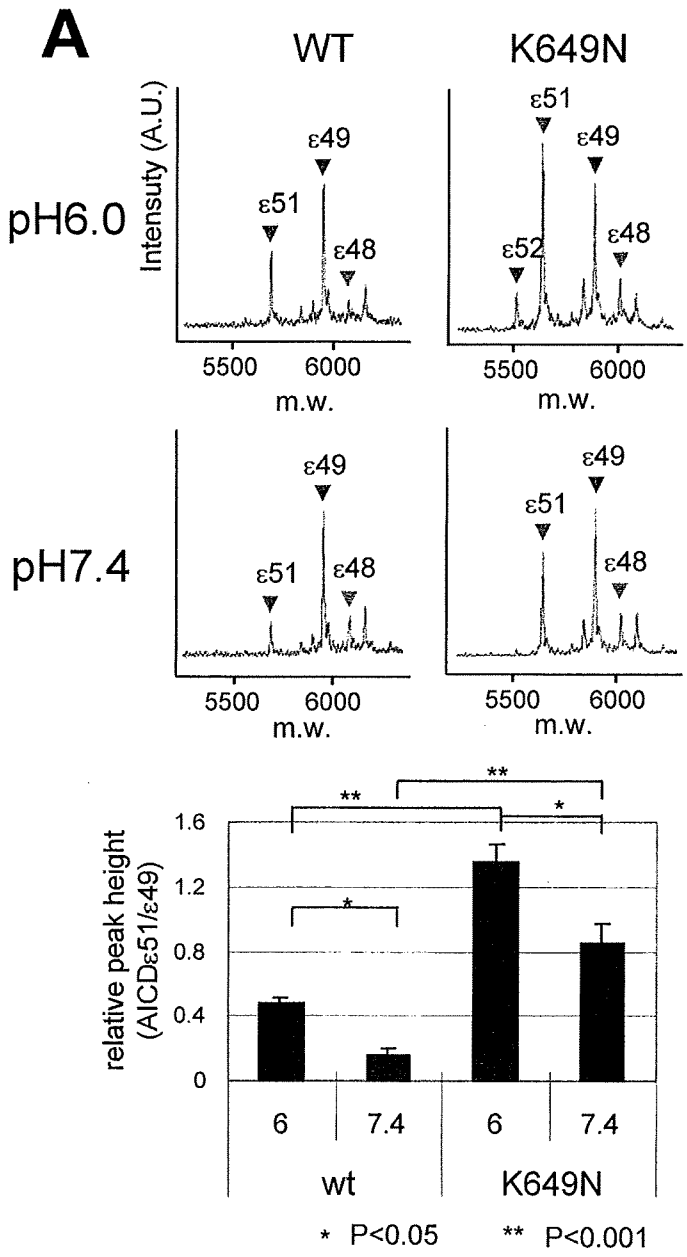

Mori et al., Figure 2

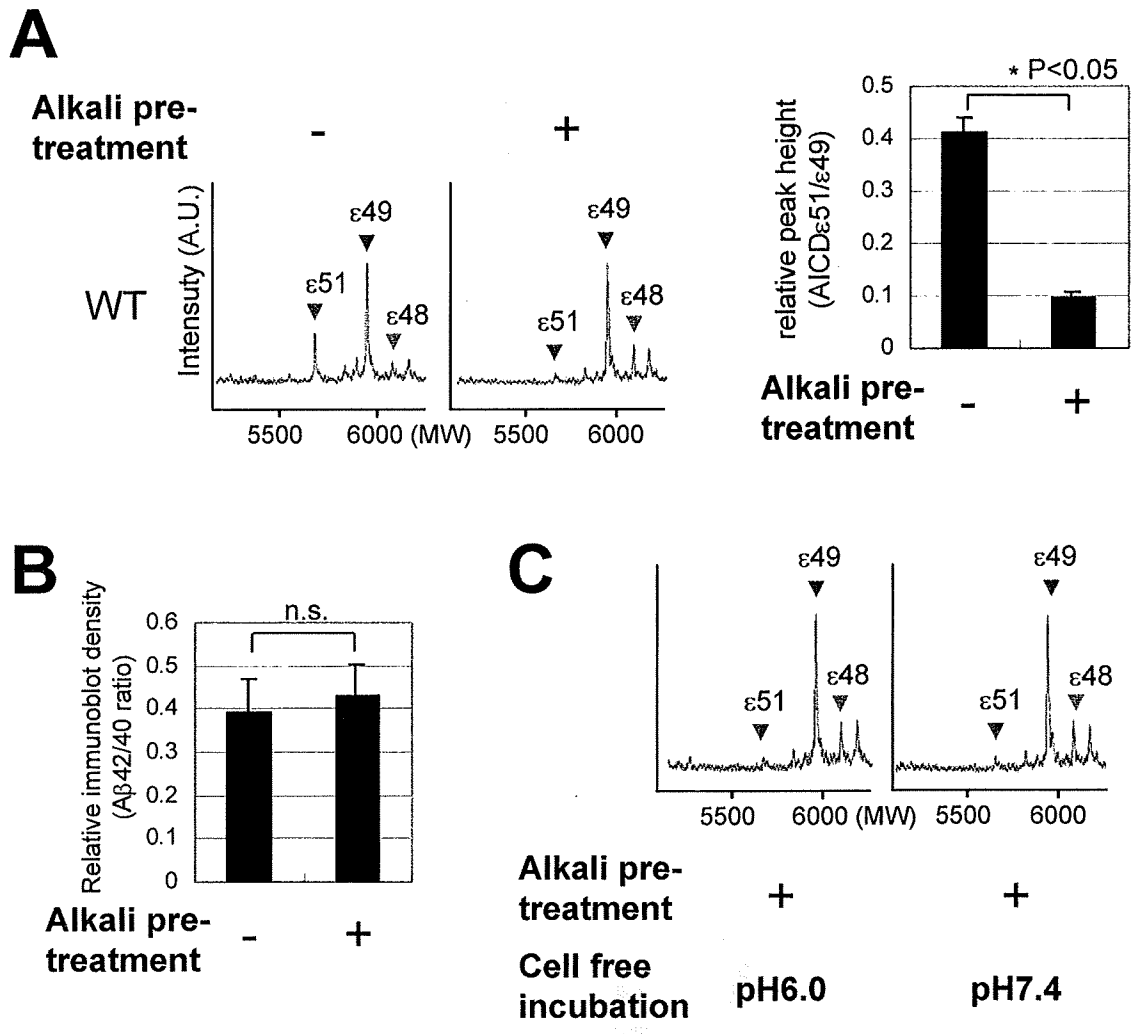

Mori et al., Figure 3